Effects of Metal Ions in the Cu_B Center on the Redox Properties of Heme in Heme-Copper Oxidases: Spectroelectrochemical Studies of an Engineered Heme-Copper Center in Myoglobin†

Xuan Zhao,‡ Natasha Yeung,‡ Zhilin Wang,§ Zijian Guo,§ and Yi Lu*,‡

Department of Chemistry, University of Illinois at Urbana-Champaign, Urbana, Illinois 61801, and Coordination Chemistry Institute, Nanjing University, Nanjing 210093, P. R. China

Received September 26, 2004; Revised Manuscript Received October 25, 2004

ABSTRACT: The electrochemical properties of an engineered heme-copper center in myoglobin have been investigated by UV−visible spectroelectrochemistry. In the cyanide-bridged, spin-coupled heme-copper center in an engineered myoglobin, the presence of Zn(II) in the Cu_B center raises the heme reduction potential from −85 to 49 mV vs NHE. However, in the cyanide-free, spin-decoupled derivative of the same protein, the presence of Zn(II) in the Cu_B center exerts little influence on the heme reduction potentials (77 and 80 mV vs NHE, respectively, in the absence and in the presence of Zn(II)). Similar trends have also been observed when copper ion is present in the Cu_B center, although on a smaller scale, due to reduction of Cu(II) to Cu(I) prior to heme reduction. These results show that the presence of a metal ion in the designed Cu_B center has a significant effect on the redox potential of heme Fe only when the two metal centers are coupled through a bridging ligand between the two metal centers, indicating that spin coupling plays an important role in redox potential regulation. In addition, the presence of a single positively charged Cu(I) center in the Cu_B center resulted in a much lower increase (16 mV) in heme reduction potential than that of two positively charged Zn(II) (118 mV). Therefore, the heme reduction potential must be lowered after the first electron transfer to reduce heme Fe^{3+}-Cu_B^{2+} to Fe^{3+}-Cu_B^{+}. To raise the heme reduction potential to make the second electron transfer (i.e., reduction of Fe^{3+}-Cu_B^{+} to Fe^{2+}-Cu_B^{+}) to be favorable, most likely a proton or decoupling of the heme-copper center is needed in the heme-copper site. These findings provide a strong argument for a thermodynamic driving force basis for redox-regulated proton transfer in heme-copper oxidases.

The heme-copper center (Figure 1A) is at the heart of the terminal oxidases, generally called heme-copper oxidases (HCO),[1] that catalyze reduction of O_2 to H_2O and transform the energy from the reaction into proton gradients for ATP synthesis (*1*−*4*). The catalytic cycle is believed to start from the oxidized state (state **O**), where the heterobinuclear center remains in oxidized forms, heme Fe^{3+}-Cu_B^{2+}. One electron reduction of state **O** leads to state **E** with a mixed valent binuclear center. State **E** can exist in the form of heme Fe^{3+}-Cu_B^{+}, heme Fe^{2+}-Cu_B^{2+}, or a form in which an electron is distributed between heme a_3 and Cu_B in rapid equilibrium. The second electron reduction of state **E** yields state **R**, the fully reduced form (heme Fe^{2+}-Cu_B^{+}) which can bind O_2 and produce state **A**. The decay of state **A** forms state $\mathbf{P_M}$ (or $\mathbf{P_R}$), with a ferryl heme iron and cupric Cu_B. The state

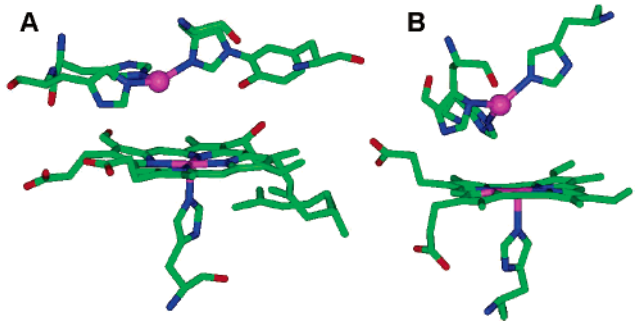

FIGURE 1: (A) Crystal structure of heme-copper center of bovine heart C*c*O (*10*). (B) The active site of a computer model of Cu_B-Mb.

$\mathbf{P_M}$ (or $\mathbf{P_R}$) is then converted to state **F** by the transfer of electron. Finally, another electron reduces state **F** to state **O**, completing the catalytic cycle (*1*−*4*). This four-electron reduction process is coupled to proton translocations; four protons are converted to H_2O, while four additional protons are pumped across the membrane.

Understanding the redox properties of the heme-copper center is essential to elucidate the redox-driven proton translocation process (*5*−*7*). A particularly interesting question is how the presence of metal ion in the Cu_B center influences redox properties of the nearby heme center that is ∼4.5 Å away (*8*−*10*). An effective approach to addressing

† This material is based on work supported by National Institutes of Health Grant GM62211.

* To whom correspondence should be addressed: Department of Chemistry, University of Illinois at Urbana-Champaign, Urbana, IL 61801. Phone: (217) 333 2619. Fax: (217) 333 2685. E-mail: yi-lu@uiuc.edu.

‡ Department of Chemistry, University of Illinois at Urbana-Champaign.

§ Coordination Chemistry Institute, Nanjing University.

[1] Abbreviations: HCO, heme-copper oxidases; Mb, myoglobin; swMb, sperm whale myoglobin; Cu_BMb, F43H/L29HswMb; WT, wild type.

10.1021/bi0479151 CCC: $30.25
Published on Web 01/06/2005

this question is through metal ion substitution, an approach that has been shown to be successful in addressing similar questions in other proteins (*11*−*13*). By comparing redox properties of the heme when the Cu_B site is metal-free, or occupied by either redox-active or redox-inactive metal ions of different oxidation states, one can reveal the subtle role the Cu_B center plays in the heme-copper center. Unfortunately, it has been difficult to define reduction potentials of each metal center in heme-copper oxidases due to the presence of several redox-active centers and their interactions. Although derivatives where Cu_B is removed or substituted by other metal ions have been prepared (for recent examples, see refs *14* and *15*), the role of Cu_B in influencing reduction potentials of the heme center remains to be addressed.

An alternative approach to addressing the above question is through the study of model heme-copper systems where the dinuclear center is free of other redox-active centers (*16*−*18*). A successful example of using the metal substitution approach has been reported for a heme-copper synthetic model system (*19*). Interestingly, the study showed that the presence of a positively charged copper ion resulted in <20 mV of heme reduction potential increase in this synthetic model system. On the other hand, it has been reported that the presence of charged amino acid residues in the heme binding pocket can change the reduction potentials of the heme by up to 200 mV (*20*).

To gain a deeper insight into this question of the role of metal ion in the Cu_B center on the reduction potential of heme, we carried out spectroelectrochemical studies of an engineered heme-copper center in sperm whale myoglobin (F43H/L29HswMb, called Cu_BMb, Figure 1B) (*21*). Myoglobin (Mb) is one of the most well-characterized heme proteins. It has been proposed that several states in HCOs, such as oxy state **A**, have analogous counterparts in Mb. Therefore, we engineered a Cu_B center in the corresponding location of sperm whale Mb and demonstrated that the Cu_B and proton play important roles in the HCO activities (*22*). This model heme-copper protein is valuable because it is easy to construct, purify, and crystallize the protein, its mutants, and other variants where the heme or Cu_B center is substituted by other types of heme or metal ions, respectively. Here we report further study of this model protein by spectroelectrochemistry. Results from this study indicate that, while a metal ion in the Cu_B site exerts only a small influence on the heme reduction potential when it is not coupled to the heme iron center, it can dramatically increase the heme reduction potential when it is coupled to the heme iron. This metal ion-dependent redox control could be a key factor in proton coupled electron transfer at the heme-copper center.

EXPERIMENTAL METHODS

The WTswMb and Cu_BMb proteins were expressed and purified as described previously. Phenazine methosulfate and anthraquinone-2-sulfonate were obtained from Sigma. The reduction potentials were measured by a spectroelectrochemical method using an optically transparent thin layer cell (OTTLE) as described in detail by Crumbliss, A. L., et al. (*23*). The working electrode is made from a piece of 52 mesh platinum gauze. A 1-mm diameter platinum wire was used as the auxiliary electrode, while a piece of Pasteur pipet filled with agar gel containing 0.5 M KNO_3 was used as salt bridge to connect the Ag/AgCl (3 M KCl) reference electrode to the bulk solution containing the working and auxiliary electrodes. Generally, the redox titration was performed using ~0.6 mL of working solution containing 0.2 mM protein, 40 μM phenazine methosulfate, and 40 μM anthraquinone-2-sulfonate as mediators. The working solution was purged gently with Ar for at least 30 min to remove O_2 before being transferred to the OTTLE cell.

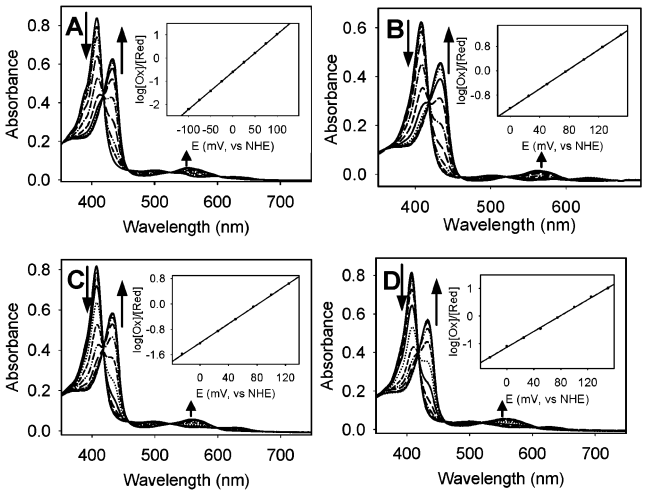

FIGURE 2: Spectroelectrochemical titration in 50 mM MOPS, pH 8 at 25 °C for (A) WTswMb (0.2 mM); (B) Cu_BMb (0.2 mM); (C) Cu_BMb in the presence of 2 equiv of Cu(II) (0.4 mM) and (D) Cu_BMb in the presence of 2 equiv of Zn(II) (0.4 mM). (Inset) Nernst plot for the dependence of the absorbance at 431 nm on the applied potential. The sweep potentials were applied in the negative direction.

A model 362 potentiostat from Princeton Applied Research was used to control the potential of the working electrode. After potential (typically with 25 mV increments) was applied, the UV−vis spectra were recorded using a Cary 3E spectrophotometer until no further spectral changes occurred. The Ag/AgCl (3 M KCl) reference electrode was calibrated with a SCE electrode and found to be 200 mV (vs NHE).

Data Analysis. The spectroelectrochemical titration data for the entire spectra were analyzed by global analysis using singular value decomposition (SVD) and nonlinear regression modeling with SpecFit/32 (Spectrum Software Associates, Inc). With the exception of redox titrations of CN^--bridged Cu_BMb−CN−Cu, all the data were fit with a model of A ↔ B because a Nernst plot at a single wavelength (e.g., 431 nm) is linear (see Figure 2). For redox titrations of CN^--bridged Cu_BMb−CN−Cu, a Nernst plot at a single wavelength (e.g., 431 nm) is nonlinear (see Figure 3C). Therefore, a model of A ↔ B ↔ C was used. The reduction potential of each protein was then obtained from the Nernst plot by plotting the applied potential vs the logarithm of the ratio of the oxidized to reduced forms of the protein from the global analysis of the entire spectra described above. Data analysis using a single wavelength (such as 431 nm) instead of the entire spectra resulted in the same reduction potential within the error of the analysis (typically ±3 mV).

RESULTS AND DISCUSSION

The spectra from spectroelectrochemical reduction of WTswMb in 50 mM MOPS at pH 8 are shown in Figure 2A. On the basis of a Nernst plot for the dependence of the

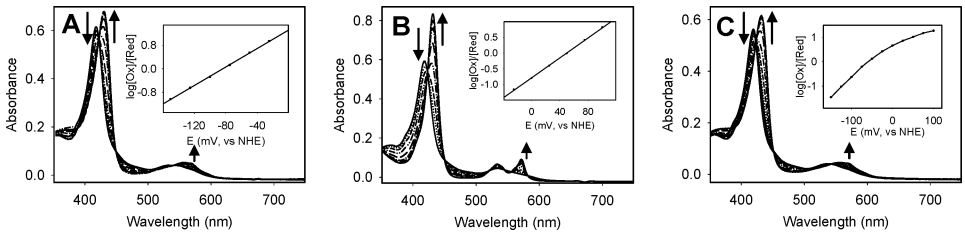

FIGURE 3: Spectroelectrochemical titration of (A) Cu_BMb-CN; (B) $Cu_BMb-CN-Zn$; and (C) $Cu_BMb-CN-Cu$ solutions (Cu_BMb, 0.2 mM; KCN, 10 mM; Cu or Zn; 1 mM) in 200 mM MOPS, pH 8 at 25 °C using phenazine methosulfate (40 μM) and anthraquinone-2-sulfonate (40 μM) as mediators. (Inset) Nernst plot from the dependence of the absorbance at 431 nm on the applied potential. The sweep potentials were applied in the negative direction.

Scheme 1: Redox-Coupled Proton Transfer Reactions in Heme a_3-Cu_B Center of HCO

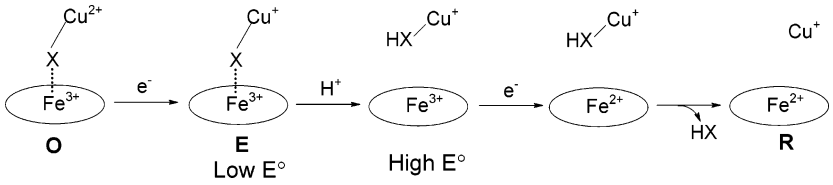

absorbance at 431 nm on the applied potential (Figure 2A, inset), the midpoint potential of WTswMb was found to be 37 mV (vs NHE). This potential is similar to that obtained by oxidation−reduction titration of WTswMb (40 mV vs NHE) (*23*, *24*). Under identical conditions, the spectra from spectroelectrochemical reduction of copper-free met-Cu_BMb were obtained (see Figure 2B). The midpoint potential of copper-free Cu_BMb was found to be 77 mV (vs NHE), indicating that mutation of L29 and F43 to histidines in swMb led to an increase of 40 mV in the heme reduction potential. Interestingly, addition of Cu(II) to Cu_BMb resulted in a very similar midpoint potential of the heme center (80 mV) (Figure 2C). This result is consistent with the previous observation in a synthetic model system (*19*). Because the copper ion is redox active and may play a role in redox titration of the heme, we carried out the same experiment in the presence of Zn(II), a redox inactive mimic of Cu(II) (Figure 2D). The same reduction potential (80 mV) was obtained.

To probe further the role of metal ions in the Cu_B center on the reduction potential of the heme when a diatomic ligand is present, we measured reduction potentials of the heme in cyanometMb. As shown in Figure 3A, the reduction potential of heme Fe in the copper-free cyanomet-Cu_BMb was determined to be −85 mV (vs NHE) from the Nernst plot at 431 nm. This potential is ∼265 mV higher than that of cyanomet-WTswMb (−350 mV vs NHE, measured in this work under identical conditions). In wild-type horse heart myoglobin, introduction of a histidine group (V68H) in the heme distal pocket was shown to increase the heme reduction potential by 128 mV in the cyanometMb (from −385 to −257 mV vs NHE) (*25*, *26*). This increase in reduction potential was attributed to stabilization of the reduced form of cyanometMb by the histidine (*25*, *26*). In Cu_BMb, two more histidine residues are present in the heme distal pocket in comparison to WTswMb, making the reduced form of cyanomet-Cu_BMb even more stable. Therefore, such a large increase in reduction potential in cyanomet-Cu_BMb is reasonable.

The most interesting results from this investigation are the strong influence of metal ions in the Cu_B center on the heme reduction potentials in the cyanomet-Cu_BMb. Unlike the cyano-free derivative, redox titration of cyanomet-Cu_BMb in the presence of Zn(II) showed a dramatic increase in heme potential from −85 to 49 mV. In the presence of Cu(II), the spectroelectrochemical titration of cyanomet-Cu_BMb showed a nonlinear Nernst plot (Figure 3C). Two reduction potentials with $E_1 = 45$ mV and $E_2 = -69$ mV were obtained by fitting the data from the entire spectra to a system involving two consecutive electron-transfer reactions. The higher reduction potential (E_1) can be assigned to the reduction of Cu(II) to Cu(I) in the CN^--bridged heme Fe−CN−Cu center, while the lower reduction potential E_2 can be assigned as the heme Fe midpoint potential, because the Cu(II)/Cu(I) redox couple normally possesses a higher reduction potential than heme in Mb. In addition, from the spectra changes displayed in Figure 3C, the heme is not fully reduced until the second process is complete, supporting the assignment that the first redox process is not directly linked to heme reduction. This heme midpoint potential in the presence of copper (−69 mV vs NHE) is lower than that in the presence of Zn(II) (49 mV vs NHE), and yet is still higher than that in the absence of metal ions (−85 mV vs NHE).

Table 1: Reduction Potentials of Heme in the Heme-Copper Center of Cu_BMb

$E_{1/2}(Fe^{III}/Fe^{II})$ (mV, vs NHE)	CN^--free	CN^--bound
no M(II)	77	−85
Cu(II)	80	−69
Zn(II)	80	49

So why do zinc and copper ions exert little effects on the reduction potentials of heme in the cyanide-free met-Cu_BMb, while they have significant effects in the cyanomet-Cu_BMb? Spectroscopic studies have shown that the engineered Cu_BMb binds a single copper ion in the Cu_B center in both cyano-free- and cyanomet-Cu_BMb (*21*). The spectroelectrochemical titrations in this study were carried out under saturating concentration of Cu(II), Zn(II), and cyanide. Therefore, lack of metal ion binding or difference in metal-binding affinity can be ruled out as the difference in heme reduction potentials.

A previous report has shown no spin coupling between Cu(II) and heme in cyanide-free met-Cu_BMb and strong

coupling in the cyanomet-Cu_BMb, indicating that the copper or zinc ions interact with heme only through space in the cyanide-free met-Cu_BMb, while they interact with heme through the CN^--bridge in the cyanomet-Cu_BMb (*21*). Since Zn(II) is redox inactive, the formation of Cu_BMb−CN−Zn(II) places two positive charges near the heme center of Cu_BMb−CN, increasing the heme potential (see Table 1). As Cu(II) is redox active, the reduction of Cu(II) to Cu(I) leaves one positive charge on the Cu_BMb−CN center, lowering the heme reduction potential by 118 mV in comparison to its Zn(II) analogue. Because of the net one positive charge, it is still 16 mV higher than that of Cu_B-free cyanomet-Cu_BMb. Apparently, the charge on the Cu_B site metal ion within the distal heme pocket has a significant effect on the redox properties of heme Fe only when the metal ion is coupled to the heme.

For the HCOs, reduction of the heme in the heme-copper center is the key initial step in the enzymatic reaction (*1*−*4*). The reduction potential must remain higher than that of its electron donor, a low-spin heme *a* center, in order for the reaction to proceed. We have shown here that binding of a diatomic ligand such as cyanide lowers the reduction potential of the heme significantly, making it difficult to be reduced by heme *a*. One way to compensate such an effect is by the presence of Cu(II) to increase the potential of the heme. However, since Cu(II)/Cu(I) reduction potentials are normally higher than those of Fe(III)/Fe(II) hemes, Cu(II) is reduced first to Cu(I), making the effect of Cu(I) on increasing the heme potential much smaller. A similar condition will occur after the first electron transfer to the heme a_3−Cu_B center of state **O** in HCOs; the reduction potential of heme a_3 in state **E** will be lowered significantly after the input of a negative charge into the binuclear site (see Scheme 1) (*27*, *28*). Therefore, to facilitate the second electron transfer and ease of O_2 reduction, a positive charge, most likely a proton, would be required to compensate for the electron-rich Cu(I) site in the binuclear site of state **E** to increase the reduction potential of heme a_3 and thus allow the second electron to reduce heme a_3, producing state **R** (see Scheme 1). Alternatively, decoupling of the heme-copper may also increase the reduction potential of the heme since we have shown that the reduced charge in the copper center will not affect the heme potential when the heme-copper centers are not coupled. Earlier reports have suggested that reduction of heme a_3 is coupled to the protonation of a group close to the heme a_3−Cu_B binuclear site in the native HCOs, probably a OH^- ligand bound to Cu_B center (*29*−*35*). This protonation can result in a more positive charge in the dinuclear center, decoupling of the heme-copper center, or both, and thus can raise the heme potential for the second electron transfer. The electrochemical studies presented here provide a strong thermodynamic driving force basis for such a proposal.

CONCLUSIONS

In summary, the redox titration of the heme-copper centers in the engineered Cu_BMb showed that the redox properties of the heme Fe depend strongly on the surrounding environment and electrostatic changes within the heme distal pocket. The presence of a metal ion in the Cu_B site has a significant effect on the redox properties of heme only when the two metal centers are coupled, suggesting a significant role of spin coupling in regulating reduction potentials of the heme-copper center. Furthermore, since the singly positively charged Cu(I) results in much less increase of reduction potential of heme than the doubly positively charged Cu(II), the redox-coupled proton transfer may be crucial to regulating the reduction potential of heme a_3 during enzyme catalysis.

ACKNOWLEDGMENT

We thank Dr. Ju Chou and Professor Hiroyasu Tachikawa from the Jackson State University for initial cyclic voltammetry studies, Professor Takashi Hayashi and Dr. Joel E. Morgan for advice on spectroelectrochemical cells, and Professor Andrew A. Gewirth for helpful discussions.

REFERENCES

1. Babcock, G. T., and Wikström, M. (1992) Oxygen activation and the conservation of energy in cell respiration, *Nature 356*, 301−309.
2. Garcia-Horsman, J. A., Barquera, B., Rumbley, J., Ma, J., and Gennis, R. B. (1994) The superfamily of heme-copper respiratory oxidases, *J. Bacteriol. 176*, 5587−5600.
3. Ferguson-Miller, S., and Babcock, G. T. (1996) Heme/Copper Terminal Oxidases, *Chem. Rev. 96*, 2889−2907.
4. Namslauer, A., and Brzezinski, P. (2004) Structural elements involved in electron-coupled proton transfer in cytochrome *c* oxidase, *FEBS Lett. 567*, 103−110.
5. Blair, D. F., Ellis, W. R., Jr., Wang, H., Gray, H. B., and Chan, S. I. (1986) Spectroelectrochemical study of cytochrome *c* oxidase: pH and temperature dependences of the cytochrome potentials. Characterization of site−site interactions, *J. Biol. Chem. 261*, 11524−11537.
6. Hendler, R. W. and Westerhoff, H. V. (1992) Redox interactions in cytochrome *c* oxidase: from the "neoclassical" toward "modern" models, *Biophys. J. 63*, 1586−1604.
7. Hellwig, P., Grzybek, S., Behr, J., Ludwig, B., Michel, H., and Maentele, W. (1999) Electrochemical and Ultraviolet/Visible/Infrared Spectroscopic Analysis of Heme a and a_3 Redox Reactions in the Cytochrome *c* Oxidase from Paracoccus denitrificans: Separation of Heme a and a_3 Contributions and Assignment of Vibrational Modes, *Biochemistry 38*, 1685−1694.
8. Iwata, S., Ostermeier, C., Ludwig, B., and Michel, H. (1995) Structure at 2.8 Å resolution of cytochrome *c* oxidase from *Paracoccus denitrificans*, *Nature 376*, 660−669.
9. Tsukihara, T., Aoyama, H., Yamashita, E., Tomizaki, T., Yamaguchi, H., Shinzawa-Itoh, K., Nakashima, R., Yaono, R., and Yoshikawa, S. (1995) Structures of metal sites of oxidized bovine heart cytochrome *c* oxidase at 2.8 Å, *Science 269*, 1069−1074.
10. Yoshikawa, S., Shinzawa-itoh, K., Nakashima, R., Yaono, R., Yamashita, E., Inoue, N., Yao, M., Fei, M. J., Libeu, C. P., Mizushima, T., Yamaguchi, H., Tomizaki, T., and Tsukihara, T. (1998) Redox-coupled crystal structural changes in bovine heart cytochrome *c* oxidase, *Science 280*, 1723−1729.
11. Vila, A. J., and Fernandez, C. O. (1996) Structure of the Metal Site in Rhus vernicifera Stellacyanin: A Paramagnetic NMR Study on its Co(II) Derivative, *J. Am. Chem. Soc. 118*, 7291−7298.
12. Hay, M. T., Milberg, R. M., and Lu, Y. (1996) Preperation and Characterization of Mercury and Silver Derivatives of an Engineered Purple Copper Center in Azurin, *J. Am. Chem. Soc. 118*, 11976−11977.
13. Lyons, T. J., Nersissian, A., Huang, H., Yeom, H., Nishida, C. R., Graden, J. A., Gralla, E. B., and Valentine, J. S. (2000) The metal binding properties of the zinc site of yeast copper−zinc superoxide dismutase: implications for amyotrophic lateral sclerosis, *J. Biol. Inorg. Chem. 5*, 189−203.
14. Hellwig, P., Pfitzner, U., Behr, J., Rost, B., Pesavento, R. P., von Donk, W., Gennis, R. B., Michel, H., Ludwig, B., and Maentele, W. (2002) Vibrational Modes of Tyrosines in Cytochrome *c* Oxidase from *Paracoccus denitrificans*: FTIR and Electrochemical Studies on Tyr-D4-labeled and on Tyr280His and Tyr35Phe Mutant Enzymes, *Biochemistry 41*, 9116−9125.
15. Das, T. K., Pecoraro, C., Tomson, F. L., Gennis, R. B., and Rousseau, D. L. (1998) The Post-translational Modification in Cytochrome *c* Oxidase Is Required To Establish a Functional Environment of the Catalytic Site, *Biochemistry 37*, 14471−14476.

16. Lu, Y., Berry, S. M., and Pfister, T. D. (2001) Engineering novel metalloproteins: Design of metal-binding sites into native protein scaffolds, *Chem. Rev. 101*, 3047−3080.
17. Collman, J. P., Boulatov, R., Sunderland, C. J., and Fu, L. (2004) Functional Analogues of Cytochrome *c* Oxidase, Myoglobin, and Hemoglobin, *Chem. Rev. 104*, 561−588.
18. Kim, E., Chufan, E. E., Kamaraj, K., and Karlin, K. D. (2004) Synthetic Models for Heme-Copper Oxidases, *Chem. Rev. 104*, 1077−1133.
19. Boulatov, R., Collman, J. P., Shiryaeva, I. M., and Sunderland, C. J. (2002) Functional Analogues of the Dioxygen Reduction Site in Cytochrome Oxidase: Mechanistic Aspects and Possible Effects of CuB, *J. Am. Chem. Soc. 124*, 11923−11935.
20. Varadarajan, R., Zewert, T. E., Gray, H. B., and Boxer, S. G. (1989) Effects of buried ionizable amino acids on the reduction potential of recombinant myoglobin, *Science 243*, 69−72.
21. Sigman, J. A., Kwok, B. C., and Lu, Y. (2000) From Myoglobin to Heme-Copper Oxidase: Design and Engineering of a Cu_B Center into Sperm Whale Myoglobin, *J. Am. Chem. Soc. 122*, 8192−8196.
22. Sigman, J. A., Kim, H. K., Zhao, X., Carey, J. R., and Lu, Y. (2003) The role of copper and protons in heme-copper oxidases: Kinetic study of an engineered heme-copper center in myoglobin, *Proc. Natl. Acad. Sci., U.S.A. 100*, 3629−3634.
23. Taboy, C. H., Bonaventura, C., and Crumbliss, A. L. (2002) Anaerobic oxidations of myoglobin and hemoglobin by spectroelectrochemistry, *Methods Enzymol. 353*, 187−209.
24. Brunori, M., Saggese, U., Rotilio, G. C., Antonini, E., and Wyman, J. (1971) Redox equilibrium of sperm-whale myoglobin, Aplysia myoglobin, and Chironomus thummi hemoglobin, *Biochemistry 10*, 1604−1609.
25. Lloyd, E., King, B. C., Hawkridge, F. M., and Mauk, A. G. (1998) Electrostatic Modulation of Ligand Binding and Electrochemical Properties of Myoglobin: The Role of Charge Compensation, *Inorg. Chem. 37*, 2888−2892.
26. King, B. C., Hawkridge, F. M., and Hoffman, B. M. (1992) Electrochemical studies of cyanometmyoglobin and metmyoglobin: implications for long-range electron transfer in proteins, *J. Am. Chem. Soc. 114*, 10603−10608.
27. Kannt, A., Lancaster, C. R. D., and Michel, H. (1998) The role of electrostatic interactions for cytochrome *c* oxidase function, *J. Bioenerg. Biomembr. 30*, 81−87.
28. Michel, H. (1999) Cytochrome *c* Oxidase: Catalytic Cycle and Mechanisms of Proton Pumping-A Discussion, *Biochemistry 38*, 15129−15140.
29. Verkhovsky, M. I., Morgan, J. E., and Wikstroem, M. (1995) Control of electron delivery to the oxygen reduction site of cytochrome *c* oxidase: A role for protons, *Biochemistry 34*, 7483−7491.
30. Aedelroth, P., Sigurdson, H., Hallen, S., and Brzezinski, P. (1996) Kinetic coupling between electron and proton transfer in cytochrome *c* oxidase: simultaneous measurements of conductance and absorbance changes, *Proc. Natl. Acad. Sci. U.S.A. 93*, 12292−12297.
31. Aedelroth, P., Brzezinski, P., and Malmstroem, B. G. (1995) Internal Electron Transfer in Cytochrome *c* Oxidase from *Rhodobacter sphaeroides*, *Biochemistry 34*, 2844−2849.
32. Juenemann, S., Meunier, B., Gennis, R. B., and Rich, P. R. (1997) Effects of Mutation of the Conserved Lysine-362 in Cytochrome *c* Oxidase from *Rhodobacter sphaeroides*, *Biochemistry 36*, 14456−14464.
33. Karpefors, M., Adelroth, P., Aagaard, A., Sigurdson, H., Ek, M. S., and Brzezinski, P. (1998) Electron−proton interactions in terminal oxidases, *Biochim. Biophys. Acta 1365*, 159−169.
34. Fann, Y. C., Ahmed, I., Blackburn, N. J., Boswell, J. S., Verkhovskaya, M. L., Hoffman, B. M., and Wikström, M. (1995) Structure of Cu_B in the Binuclear Heme-Copper Center of the Cytochrome aa_3-Type Quinol Oxidase from Bacillus subtilis: An ENDOR and EXAFS Study, *Biochemistry 34*, 10245−10255.
35. Braenden, M., Namslauer, A., Hansson, O., Aasa, R., and Brzezinski, P. (2003) Water-Hydroxide Exchange Reactions at the Catalytic Site of Heme-Copper Oxidases, *Biochemistry 42*, 13178−13184.

BI0479151